MATHEMATICAL BIOSCIENCES
AND ENGINEERING
Volume **1**, Number **1**, June **2004**

http://math.asu.edu/~mbe/

pp. **61–80**

ON DERIVING LUMPED MODELS FOR BLOOD FLOW AND PRESSURE IN THE SYSTEMIC ARTERIES

Mette S. Olufsen

Department of Mathematics
North Carolina State University
Box 8205
Raleigh, NC 27695
Edwardsville, Illinois, 62026-1653

Ali Nadim

Keck Graduate Institute
535 Watson Drive
Claremont, CA 91711

(Communicated by James F. Selgrade)

Abstract. Windkessel and similar lumped models are often used to represent blood flow and pressure in systemic arteries. The windkessel model was originally developed by Stephen Hales (1733) and Otto Frank (1899) who used it to describe blood flow in the heart. In this paper we start with the one-dimensional axisymmetric Navier-Stokes equations for time-dependent blood flow in a rigid vessel to derive lumped models relating flow and pressure. This is done through Laplace transform and its inversion via residue theory. Upon keeping contributions from one, two, or more residues, we derive lumped models of successively higher order. We focus on zeroth, first and second order models and relate them to electrical circuit analogs, in which current is equivalent to flow and voltage to pressure. By incorporating effects of compliance through addition of capacitors, windkessel and related lumped models are obtained. Our results show that given the radius of a blood vessel, it is possible to determine the order of the model that would be appropriate for analyzing the flow and pressure in that vessel. For instance, in small rigid vessels ($R < 0.2$ cm) it is adequate to use Poiseuille's law to express the relation between flow and pressure, whereas for large vessels it might be necessary to incorporate spatial dependence by using a one-dimensional model accounting for axial variations.

1. **Introduction and background.** Windkessel and similar lumped models are often used to represent blood flow and pressure in the arterial system [4, 26, 29, 34]. These lumped models can be derived from electrical circuit analogies where current represents arterial blood flow and voltage represents arterial pressure. Resistances represent arterial and peripheral resistance that occur as a result of viscous dissipation inside the vessels, capacitors represent volume compliance of the vessels that allows them to store large amounts of blood, and inductors represent inertia of the blood. The windkessel model was originally put forward by Stephen Hales in 1733 [13] and further developed by Otto Frank in 1899 [11]. Frank used the

2000 *Mathematics Subject Classification.* 76205, 92C35.
Key words and phrases. Arterial modeling, Lumped arterial models.

windkessel model to describe blood flow in the heart and systemic arteries. He used the analogy of an old-fashioned hand-pumped fire engine (in German "windkessel" pump). Firemen pump water into a high-pressure air-chamber by periodic injections at high pressure. When the air-chamber is full, the high pressure drives the water out in a steady jet. This analogy starts at the left ventricle where the blood pressure varies from a low of nearly zero to a high of approximately 120 mmHg and continues into the aorta and the systemic arteries where the pressure variation is significantly less because of the elasticity of the large systemic arteries. This analogy resulted in the development of the original (two-element) windkessel model comprising an electrical circuit with one resistor and one capacitor.

Even though the model was originally derived for the ventricle and the aorta, it was also used to describe blood flow in the systemic arteries alone (i.e. without explicitly including the heart); in this case the capacitor represents the compliance of the large arteries while the resistor represents the resistance of the small arteries and arterioles (so-called resistance vessels). The two-element windkessel model was later extended to the three-element windkessel model, which has two resistors and a capacitor. In this model, the additional resistor is thought to represent the characteristic impedance of the aorta and the large compliance vessels. The three-element windkessel model is widely used, and it produces realistic blood flow and pressure wave shapes as well as estimates experimental data [7, 10, 16, 21, 28, 30, 35]. Further expansions of the windkessel model into a four-element model have proven even better at getting good comparisons between measured blood flow and pressure. In addition to the two resistors and the capacitor of the three-element windkessel model, the four-element model includes an inductor representing the inertia of the blood [16, 29, 31]. The advantage of lumped models is that they are easy to understand and solve, since they give rise to simple ordinary differential equations. However, these models include a number of parameters (resistors, capacitors, and inductors), and it is not obvious how to estimate the parameters from measurements of arterial blood flow and pressure [21, 25, 29].

In general, blood flow in arteries is a pulsatile flow in tapered elastic vessels that are connected in a branching network [5, 14, 19, 20, 24, 27]. Blood flow is unsteady, and the fluid is non-Newtonian. So, to develop a complete model for blood flow in arteries, these effects should be taken into account. That is, one would have to use the full theory of fluid dynamics, which requires solving the Navier-Stokes (NS) equations, together with appropriate non-Newtonian constitutive relations for blood, coupled with the dynamics of the compliant vessels through which blood flows. For the large arteries, blood can usually be modelled as incompressible and Newtonian; nevertheless, to study blood flow in detail, it is still necessary to solve the NS equations.

The disadvantage of working with the full non-linear NS equations is that, even if only one spatial dimension (axial) is taken into account, it is significantly more difficult to set up a system of equations predicting the blood flow and pressure in all of the large systemic arteries [19, 20]. In addition, while such one-dimensional models provide insight into wave-propagation and some of the non-linear dynamics, they are not useful for answering questions aimed at understanding the global behavior of the system. One-dimensional models can be obtained by assuming that the vessels are axisymmetric and that the velocity profile across the vessel diameter is known [5, 14, 19, 20, 27].

There are many applications, however, where it would be important to be able to solve the model equations for blood flow in arteries in real time; e.g., in the development of anesthesia simulators [17], where a mathematical model of the cardiovascular system is used in conjunction with various pharmaco-kinetic and dynamic models. In such cases, use of lumped models provides a distinct advantage. Other reasons for using lumped models instead of the NS equations to analyze data that include dynamic changes, such as those associated with posture change from sitting to standing [21], or baroreceptor regulation [9, 22, 23, 32, 33]; finally such models are useful because they are easy to implement in a clinical setting.

Womersley was the first person to study blood flow in arteries using a linearized version of the NS equations [36, 37]. This system of equations is discussed further by Atabek, Lew, and Gessner in [2, 3, 12]. The approach used in this paper is based on the ideas outlined by Gessner [12] and Berger [5] with the aim of comparing the windkessel model with the fluid dynamic equations.

In the present work we use the equations of fluid dynamics to derive a number of lumped models for blood flow and pressure in the systemic arteries. More precisely, starting with the one-dimensional NS equations describing time-dependent flow and pressure in a rigid vessel, we derive first- and second-order lumped models using Laplace transform, residue theory, and solutions to a Bessel equation. In the inversion step of the Laplace transform, by including the residues from more and more poles, we can obtain successively higher-order models. The resulting lumped models can be represented by electrical circuits. It should be noted that the immediate interpretation of these lumped circuits has to be for the particular vessel for which the one-dimensional model was derived. We show that the differential equations representing the windkessel model have the same form as those obtained from a first-order approximation of the fluid dynamics equations for flow in a rigid vessel, but that the parameters must be interpreted somewhat differently. The novelty in our approach compared to earlier work is that by using the Laplace transform and residue theory, we obtain the solution exactly in the Laplace domain and we make systematic approximations only during the inversion step to derive various lumped models that are appropriate to the diameter of the blood vessel being studied. Based upon these results, we can assess when it would be appropriate to treat a vessel as a lumped system and when it would be better to use a distributed (e.g., one-dimensional) model.

Our results suggest the following based on physical properties of blood: For vessels with a radius smaller than approximately 0.2 cm, effects of inertia can be neglected, and if the vessels are rigid it is adequate to use Poiseuille's simple relation between pressure drop and flow rate. For rigid vessels with a radius in the approximate range between 0.2 and 0.5 cm, either a first- or a second-order lumped model can be used to relate flow and pressure. For rigid vessels with a radius in the approximate range between 0.5 and 1.5 cm, higher-order terms should be included. A reduced second-order model would be appropriate, depending on the magnitude of the time-scales that appear within third- or higher-order models. We do not derive these higher-order models explicitly, but they can be found easily using the approach outlined in this paper. For non-rigid vessels, capacitors can be added to account for the vessel compliance. Finally, for vessels whose radii are larger than approximately 1.5 cm, it would be more appropriate to take spatial dependence into account and to model the relation between pressure and flow using a distributed (e.g., a one-dimensional) model [14, 19, 20, 24, 27].

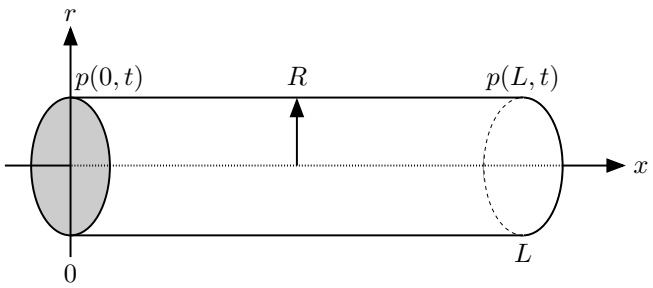

FIGURE 1. The vessel, the radius of the vessel is R and the length is L. The pressure at the inlet into the vessel is $p(0,t)$ and the pressure at the outlet is $p(L,t) = p(0,t) - (\Delta p)p^*(t)$.

In the remainder of this paper we will first discuss (in Section 2) how the Navier-Stokes equations for an incompressible and Newtonian fluid through a rigid vessel can be approximated by ordinary differential equations. In Section 3 we will describe how these ordinary differential equations can be interpreted as lumped models that can be represented by electrical circuit analogies. This section has three parts; the first part shows how our model can be represented by corresponding lumped models, the second part compares our model with the windkessel models, and the last part discusses how elasticity, represented by capacitors, can be included into the lumped models. Finally, in Section 4 we will discuss our results.

2. **Derivation of a lumped mathematical model for blood flow in arteries.** Blood flow in arteries can be modelled as a one-dimensional axisymmetric flow of an incompressible and Newtonian fluid through a rigid vessel, for which the NS equations simplify to:

$$\rho\frac{\partial u}{\partial t} + \frac{\partial p}{\partial x} = \frac{\mu}{r}\frac{\partial}{\partial r}\left(r\frac{\partial u}{\partial r}\right), \tag{1}$$

where $u(r,t)$ is the longitudinal velocity, $\rho = 1.06$ g/cm^3 is the density, $\mu = 0.049$ g/cm/s is the viscosity, and $\nu = \mu/\rho = 0.046$ cm^2/s is the kinematic viscosity of the blood. The pressure $p(x,t)$ inside the vessel is assumed to be constant over the cross-sectional area (independent of the radial coordinate r). Equation (1) describes time-dependent flow and pressure in a rigid vessel and is often referred to as Womersley's equation [36, 37]. It is obtained from the NS equations by assuming that the flow is unidirectional and axisymmetric. The assumption of unidirectional flow applies as long as the vessel is straight and sufficiently long to ignore flow disturbances at the inlet and the outlet of the vessel. Nonlinear inertial effects are absent provided that the flow remains laminar, requiring the Reynolds number to be below a critical value [8, 18, 24]. Even when the vessel is compliant, for long wavelength variations of flow and pressure, the same simplified equation approximately applies.

Our assumption of a velocity $u(r,t)$ that is independent of x gives that pressure is varies linearly with distance along the vessel (see Fig. 1). Hence, the characteristic pressure gradient can be written as

$$-\frac{\partial p}{\partial x} = \frac{p(0,t) - p(L,t)}{L} = \frac{\Delta p}{L}p^*, \tag{2}$$

where p^* is the non-dimensional pressure gradient, Δp is the characteristic change in pressure, and L is the length of the vessel. Equation (1) can be non-dimensionalized using the following dimensionless variables:

$$t^* = \frac{t\nu}{R^2}, \qquad r^* = \frac{r}{R}, \qquad \text{and} \qquad u^*(r^*, t^*) = \frac{u(r,t)L\mu}{\Delta p R^2}. \tag{3}$$

Inserting equations (2) and (3) into equation (1) and reusing the original symbols yield

$$\frac{\partial u}{\partial t} - \frac{1}{r}\frac{\partial u}{\partial r} - \frac{\partial^2 u}{\partial r^2} = p(t).$$

This equation can be transformed into a Bessel equation that can be solved analytically using the Laplace transform

$$\mathcal{L}\{u(r,t)\} = \int_0^\infty u(r,t)\, e^{-st}\, dt = \overline{u}(r,s)$$

and the property

$$\mathcal{L}\left\{\frac{\partial u}{\partial t}\right\} = s\overline{u}(r,s) - \overline{u}(r,0).$$

The Laplace transform gives

$$\frac{d^2\overline{u}}{dr^2} + \frac{1}{r}\frac{d\overline{u}}{dr} + (i\sqrt{s})^2\overline{u} = -\overline{p}(s), \tag{4}$$

where $i = \sqrt{-1}$, $\overline{p}(s) = \mathcal{L}(p(t))$, and it is assumed that there is no flow initially (i.e. $\overline{u}(r,0) = 0$). The particular solution is

$$\overline{u}(r,s) = \frac{\overline{p}(s)}{s}.$$

The remaining homogeneous equation is equivalent to Bessel's equation:

$$y^2\frac{d^2\overline{u}}{dy^2} + y\frac{d\overline{u}}{dy} + y^2\overline{u} = 0.$$

Hence, the general solution to the differential equation (4) can be written as

$$\overline{u}(r,s) = c_1 J_0(ir\sqrt{s}) + c_2 Y_0(ir\sqrt{s}) + \frac{\overline{p}(s)}{s},$$

where c_1 and c_2 are arbitrary constant and J_0 and Y_0 are the zeroth-order Bessel functions. Since Y_0 is singular at $r = 0$, constant c_2 must be set to zero. Applying the no-slip boundary condition $\overline{u}(1,s) = 0$ makes it possible to solve for the remaining constant c_1 to yield

$$\overline{u}(r,s) = \frac{\overline{p}(s)}{s}\left(1 - \frac{J_0(ir\sqrt{s})}{J_0(i\sqrt{s})}\right). \tag{5}$$

The volumetric flow rate (or simply the flow) is defined in dimensionless form by

$$\overline{q}(s) = 2\pi\int_0^1 \overline{u}(r,s)\, r\, dr. \tag{6}$$

Inserting the velocity in equation (5) into equation (6) gives

$$\overline{q}(s) = \frac{\pi\overline{p}(s)}{s}\left(1 - \frac{2J_1(i\sqrt{s})}{i\sqrt{s}J_0(i\sqrt{s})}\right), \tag{7}$$

which can be written as

$$\overline{q}(s) = \overline{p}(s)K(s), \qquad K(s) = \frac{\pi}{s}\left(1 - \frac{2J_1(i\sqrt{s})}{i\sqrt{s}J_0(i\sqrt{s})}\right). \tag{8}$$

Computing $q(t)$ using equation (7) involves computing the inverse Laplace transform of $\overline{q}(s)$, and hence, inversion of $K(s)$. This inversion can be done using the method of residues, which requires finding the poles of $K(s)$. The inverse transform is found by closing the inversion contour integral by a semi-circle in the left half-plane and letting its radius tend to infinity, where the contribution from the semi-circle itself vanishes. To complete the inversion it is advantageous to write

$$\overline{q}(s) = \frac{K(s)}{s}[s\overline{p}(s)] = M(s)\,[s\overline{p}(s)]\,, \qquad M(s) = \frac{K(s)}{s}.$$

In the time domain the flow $q(t)$ can then be found by applying the convolution theorem

$$q(t) = \int_0^t M(t-\tilde{t})p'(\tilde{t})\,d\tilde{t} \tag{9}$$

since

$$p'(t) = \mathcal{L}^{-1}\{s\overline{p}(s)\},$$

if $p(0) = 0$. The kernel $M(t)$ is given by

$$\begin{aligned} M(t) &= \mathcal{L}^{-1}\left\{\frac{K(s)}{s}\right\} \\ &= \frac{1}{2\pi i}\int_{c-i\infty}^{c+i\infty}\frac{K(s)}{s}\,e^{st}ds \\ &= \sum \mathrm{Res}\left\{\frac{K(s)}{s}\,e^{st}\right\}. \end{aligned}$$

Upon finding the residues (see Appendix A), the kernel in the time domain is found to be given by the infinite series

$$M(t) = \frac{\pi}{8} - 4\pi\sum_{n=1}^{\infty}\frac{e^{-\beta_n^2 t}}{\beta_n^4}, \tag{10}$$

where the β_n's are the roots of the Bessel function $J_0(\beta_n) = 0$. The first few of these roots are given by $\beta_1 = 2.40483$, $\beta_2 = 5.52008$, and $\beta_3 = 8.65373$ [1]. Inserting equation (10) into the convolution integral in equation (9) gives

$$q(t) = \frac{\pi}{8}p(t) - 4\pi\sum_{n=1}^{\infty}\frac{1}{\beta_n^4}\int_0^t e^{-\beta_n^2(t-\tilde{t})}p'(\tilde{t})\;d\tilde{t}. \tag{11}$$

This equation is one of the main results of the analysis; in the following we seek to approximate this solution to obtain a simple differential equation relating flow and pressure. A convenient way to proceed is to define

$$f_n(t) = \int_0^t e^{-\beta_n^2(t-\tilde{t})}p'(\tilde{t})\;d\tilde{t} \tag{12}$$

so that upon differentiation

$$f_n'(t) + \beta_n^2 f_n(t) = p'(t). \tag{13}$$

Inserting equation (12) into equation (11) gives

$$q(t) = \frac{\pi}{8}p(t) - 4\pi\sum_{n=1}^{\infty}\frac{f_n(t)}{\beta_n^4} \tag{14}$$

with each $f_n(t)$ obtained by solving equation (13). Truncating the series in equation (14) at $n = 1$ gives

$$q(t) = \frac{\pi}{8}p(t) - \frac{4\pi f_1(t)}{\beta_1^4}. \tag{15}$$

To solve equation (15), it is necessary to get an expression for $f_1(t)$. Such an expression can be found by introducing the operator $D = d/dt$ and using it to solve equation (13) for $n = 1$:

$$f_1(t) = (D + \beta_1^2)^{-1} Dp(t). \tag{16}$$

Inserting equation (16) into equation (15) and applying the operator $(D + \beta_1^2)/\beta_1^2$ to both sides of the equation gives the differential equation

$$\frac{1}{\beta_1^2}\frac{dq}{dt} + q = \frac{\pi}{8}\left(\frac{A}{\beta_1^2}\frac{dp}{dt} + p\right), \quad \text{where} \quad A = 1 - \frac{32}{\beta_1^4}. \tag{17}$$

Equation (17) can be written in the form

$$\lambda_q \frac{dq}{dt} + q = \frac{\pi}{8}\left(\lambda_p \frac{dp}{dt} + p\right), \tag{18}$$

where

$$\lambda_q = \frac{1}{\beta_1^2} \approx 0.1729 \quad \text{and} \quad \lambda_p = \frac{A}{\beta_1^2} = A\lambda_q \approx 0.0075.$$

Equation (18) has a form similar to Jeffrey's model that describes linear viscoelasticity [6] and by analogy the constant λ_q can be interpreted as the relaxation time and λ_p as the retardation time. Note that $\lambda_p \ll \lambda_q$, indicating that the change in pressure with time has a much smaller effect than the pressure itself. This equation represents the first-order model; at the end of this section, we interpret it as a lumped parameter model.

This method can also be used to obtain a second-order model by including two terms of the sum in equation (14). For the second-order method two equations of the form of equation (13) would have to be solved, one for $f_1(t)$ and one for $f_2(t)$. Similar to the first-order model, equations for these two expressions can be found using the operator method. Inserting the results into equation (14), and applying the operator $(D + \beta_1^2)(D + \beta_2^2)/\beta_1^2\beta_2^2$ to both sides of the equation yields the differential equation

$$\begin{aligned}\frac{1}{\beta_1^2\beta_2^2}\frac{d^2q}{dt^2} + \left(\frac{1}{\beta_1^2} + \frac{1}{\beta_2^2}\right)\frac{dq}{dt} + q = \frac{\pi}{8}\left\{\frac{1}{\beta_1^2\beta_2^2}\left[1 - 32\left(\frac{1}{\beta_1^4} + \frac{1}{\beta_2^4}\right)\right]\frac{d^2p}{dt^2} + \right.\\ \left.\left[\left(\frac{1}{\beta_1^2} + \frac{1}{\beta_2^2}\right) - 32\left(\frac{1}{\beta_1^6} + \frac{1}{\beta_2^6}\right)\right]\frac{dp}{dt} + p\right\}.\end{aligned} \tag{19}$$

The time-scales for the second-order model can be found by solving the characteristic polynomials for the second-order operators on each side of equation (19). In other words, writing

$$\begin{aligned} q(t) &= c_{q_1} e^{-t/\lambda_{q_1}} + c_{q_2} e^{-t/\lambda_{q_2}} \\ p(t) &= c_{p_1} e^{-t/\lambda_{p_1}} + c_{p_2} e^{-t/\lambda_{p_2}} \end{aligned}$$

as the solutions of the homogeneous differential equations obtained by setting each side of equation (19) to zero yields quadratic equations for $(1/\lambda_{q_i})$ and $(1/\lambda_{p_i})$ for $i = 1, 2$. These time-scales are similar to the retardation time and the relaxation time, except that we have two of each. Consequently, in the following we will refer to the "pressure" time-scales and the "flow" time-scales. The equation for the flow

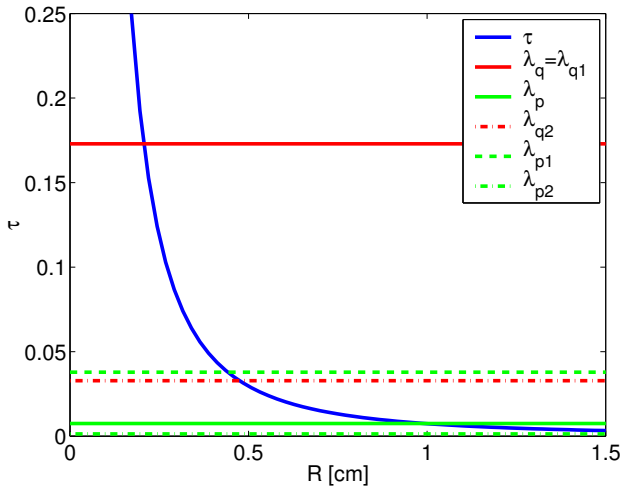

FIGURE 2. The dimensionless cardiac cycle τ (blue) as a function of the vessel radius R. The horizontal lines show the flow time-scales λ_q,λ_{q_1}, and λ_{q_2} (red) and the pressure time-scales λ_p, λ_{p_1},λ_{p_2} (green).

time-scales is easy to solve analytically, but the equation for the pressure time-scales leads to long expressions. As a result the pressure time-scales are computed numerically. The four time-scales are:

$$\lambda_{q_1} = \frac{1}{\beta_1^2} = 0.1729 \quad \lambda_{q_2} = \frac{1}{\beta_2^2} = 0.0328 \tag{20}$$
$$\lambda_{p_1} = 0.0378 \qquad \lambda_{p_2} = 0.0013.$$

An interesting observation based on examining the above results is that the second-order model for the flow includes the same time-scale λ_{q_1} as the first-order model plus an additional time-scale λ_{q_2}. The same is not the case for the pressure time-scales since both time-scales are different from the first-order model. Note that the biggest pressure time-scale for the second-order model is larger than the one obtained from the first-order model.

An important insight that can be gleaned from such derivations is related to the time-scales associated with the first (18), second (19), and higher-order equations. One can study these in relation to the characteristic time-scale of the cardiac cycle. Let the heart-rate be defined by HR so that the period of the cardiac cycle is $T = 1/\text{HR} = 1/f$ where f is the frequency. Then, the angular frequency is given by $\omega = 2\pi f$ giving a time-scale $1/\omega = T/(2\pi)$, which can be non-dimensionalized using the time-scale for t^* (see equation (3)). Thus, the dimensionless period of a cardiac cycle can be written as

$$\tau = \frac{T\nu}{2\pi R^2}.$$

Fig. 2 shows τ as a function of the vessel radius for a heart-rate of 60 beats/min (or 1 beat/sec) as well as the six different time-scales calculated thus far. The figure shows that for vessels with a radius smaller than approximately 0.2 cm, τ (blue) is larger than all flow time-scales $\lambda_q, \lambda_{q_1}, \lambda_{q_2}$ (red) and all pressure time-scales $\lambda_p, \lambda_{p_1}, \lambda_{p_2}$ (green). As a result, a time-variation of pressure on the time-scale

τ causes a change in flow that would occur almost instantaneously, the changes resulting from inertia occurring on a time-scale shorter than one cardiac cycle and therefore being almost negligible. The flow will be quasi-steady, and effects of inertia can be neglected. If the vessels are rigid, they will act as pure resistance vessels, where p is proportional to q; i.e., effects of inertia can be neglected. (Again, it should be noted that our models do not include compliance. However, if compliance is included, as discussed in Section II.C., a similar analysis of time-scales can be performed.) For these small vessels, the time derivatives in equations (18) or (19) are negligible, simplifying the equations to

$$q \approx \frac{\pi}{8} p.$$

so that we do not see any inertial effects. In dimensional form one recovers Poiseuille's relation between flow and pressure for steady laminar flow in a rigid vessel (as expected):

$$q \approx \frac{\pi R^4 p}{8 \mu L} \tag{21}$$

using

$$q^* = \frac{\mu L}{\Delta p R^4} q \quad \text{and} \quad p^* = \frac{p}{\Delta p}. \tag{22}$$

Note that the pressure $p(t)$ actually represents the pressure difference between the inlet and the outlet of the vessel (see equation (2) and Fig. 1).

Rigid vessels with a radius $R > 0.2$ cm the flow can no longer be treated as quasi-steady and it is necessary to include time-derivatives. For vessels with a radius $0.2 < R < 0.5$ cm, the time-scales that appear only in the second-order model λ_{q_2} (red dotted line), λ_{p_1}, and λ_{p_2} (green dotted lines) can be neglected, and we can approximate the flow in the vessel using the first-order model. However, since $\lambda_{q_1} > \tau$ (red solid line), terms associated with this time-scale should be included, but the time-scale dependent on λ_p (green solid line) can be neglected. Consequently, it should be sufficient to model flow in such a rigid vessel using the first-order differential equation

$$\lambda_q \frac{dq}{dt} + q = \frac{\pi}{8} p. \tag{23}$$

For vessels with a radius $R > 0.5$ cm, our analysis suggests that a second-order model would be more appropriate including all derivatives for both flow and pressure. Rewriting equation (19) in terms of the flow time-scales gives:

$$\lambda_{q_1} \lambda_{q_2} \frac{d^2 q}{dt^2} + (\lambda_{q_1} + \lambda_{q_2}) \frac{dq}{dt} + q = \frac{\pi}{8} \left(\lambda_{p_1} \lambda_{p_2} \frac{d^2 p}{dt^2} + (\lambda_{p_1} + \lambda_{p_2}) \frac{dp}{dt} + p \right). \tag{24}$$

However, since $\lambda_{p_2} \ll \lambda_{p_1}$ and since λ_{p_2} is very small, the term involving the second-order derivative in pressure will be significantly smaller than τ for vessels with a radius $0.5 < R < 1.5$ cm and may thus be neglected. (This, of course, requires the time-derivatives of pressure not to be so large as to compensate for the small coefficients in front of those derivatives. The implicit assumption is that these variations occur in a time-scale of order τ.) Finally, for the very large vessels, such as the aorta, where the radius may exceed 1.5 cm, it is necessary to include all terms for both flow and pressure time-scales. In fact, for the large vessels an even higher-order model is called for. Solely based on the time-scales λ_q, a sixth-order model would be needed to obtain a $\lambda_q < \tau$ for $R = 1.5$ cm.

In analyzing the time-scales as was undertaken above, it is worthwhile to keep the following general structure in mind. The relation between pressure and flow in the time domain ordinarily takes the form $D_1 q(t) = D_2 p(t)$ where D_1 and D_2 are linear differential operators (of successively higher order, as needed). First, one has to decide which of the two variables $q(t)$ and $p(t)$ should be regarded as input, and which as output. For instance, if $p(t)$ is taken to be the input, the right-hand side of the differential equation will be known, regardless of the time-scales appearing therein, and the equation is to be solved for $q(t)$. Normally, we regard $p(t)$ and $q(t)$ as periodic functions of time so that issues related to imposing an appropriate number of initial conditions (depending on the order of the differential operator) do not come into play. What does matter, however, is the degree to which the differential operator on each side could be reduced. The analysis of time-scales addresses this issue. For instance, if the pressure forcing is characterized by radian frequency ω, say, so that one should expect the flow response to also be characterized by the same frequency, then in each factor of the form $(1 + \lambda d/dt)$ in each differential operator, one can decide whether to keep or omit the derivative term in comparison to unity. When $\lambda\omega \ll 1$, those factors in the overall differential operators D_1 and D_2 may be replaced by unity, reducing the order of the equation. As such, by considering successively higher-order differential models, factoring the operators as products of individual terms of the form $(1+\lambda_j d/dt)$ (to within a single multiplicative constant outside these factors), and by omitting those factors for which $\lambda_j\omega$ is small in comparison to unity, one can systematically decide what the order of the appropriate model should be. An issue that complicates this analysis, however, is that for each higher-order model, the time-scales turn out to be distinct from the ones found at the previous lower order. So without actually obtaining the higher-order model, it would be hard to asses whether the lower order model is adequate. One way to avoid this complication is to use the pair of equations (13) and (14) as the starting point. Since for each n, equation (13) involves a single operator of the form $(1-\lambda_n d/dt)$ with $\lambda_n = 1/\beta_n^2$, one can determine, based on the time-scale in $p'(t)$, how many of these equations should be regarded as differential equations so that the rest can be regarded as algebraic equations directly relating $f_n(t)$ to $p'(t)$.

3. **Lumped models for arterial blood flow.**

3.1. **Derivation of lumped arterial models.**

As discussed in the introduction, a number of lumped models have been used to describe flow and pressure in the systemic arteries. The most popular of these models is the three-element windkessel model with two resistors and a capacitor (see Fig. 3D). More recently it has been suggested that addition of an inductor to the windkessel model, representing the inertia of blood, improves the agreement between the model and actual data [29].

Our derivation of the differential equation relating flow and pressure was based on modeling the NS equations for flow in a rigid vessel. As a result it is not possible to obtain lumped models that include a capacitor, but only models that include inductors and resistors representing the resistance to the flow and the inertance of the blood. Also, it should be noted, that our derivation above should be interpreted as a lumped model representing the rigid vessel it was derived for. Similar models could be obtained for any of the systemic arteries, and they could be added in series to provide a system of lumped models representing the arterial tree. Such systems have been derived and are often referred to as transmission line models.

The systems models can still be viewed from the same point of departure, since they essentially think of the entire system as flow running through one vessel with appropriate dimensions.

From the analysis in the previous section (see Fig. 2) one observes that for rigid vessels with a radius smaller than 0.2 cm, effects of inertia can be ignored and the vessels can be modelled as resistance vessels. In people, arteries of that caliber are almost rigid, so it would not be necessary to add a capacitor, only a resistor. However, if a model is constructed to study the rat aorta it is necessary to include a capacitor representing the compliance of this vessel. The circuit corresponding to these vessels is shown in Fig. 3A. The corresponding equation for this circuit is:

$$p(t) = R_1 q(t).$$

Comparing this equation with equation (21) gives $R_1 = 8\mu L/\pi R^4$. For vessels with a radius between $0.2 < R < 0.5$ cm. The flow in the vessel can be modelled using equation (23). Using the scaling factors given earlier (in equations (3) and (22)) equation (23) can be re-dimensionalized as follows

$$\frac{\lambda_q R^2}{\nu}\frac{dq}{dt} + q = \frac{\pi R^4}{8\mu L}p, \tag{25}$$

where again $p(t)$ is the pressure difference between the inlet and the outlet of the vessel, so $\partial p/\partial x = -p/L$. The above equation can be obtained from a circuit with a resistor and an inductor in series (see Fig. 3B). For this circuit the equation is:

$$\frac{L_1}{R_1}\frac{dq}{dt} + q = \frac{1}{R_1}p. \tag{26}$$

Comparing the last equation with equation (25) gives values for the inductance L_1 and the resistance R_1 as functions of the vessel and fluid properties:

$$R_1 = \frac{8\mu L}{\pi R^4} \quad \text{and} \quad L_1 = \frac{8\lambda_q \rho L}{\pi R^2}. \tag{27}$$

This result is similar to the one obtained by Stergiopulos et al. [29]. The difference is that they have a factor 4/3 instead of $8\lambda_q$, which is slightly higher. Including the retardation term (even though it is small) yields a differential equation in the form of equation (18), which in dimensional form can be written as

$$\frac{\lambda_q R^2}{\nu}\frac{dq}{dt} + q = \frac{\pi R^4}{8\mu L}\left(\frac{\lambda_p R^2}{\nu}\frac{dp}{dt} + p\right). \tag{28}$$

This differential equation can be represented by two resistors and an inductor (see Fig. 3C). For this circuit the equation is:

$$L_1\left(\frac{1}{R_1} + \frac{1}{R_2}\right)\frac{dq}{dt} + q = \frac{1}{R_2}\left(\frac{L_1}{R_1}\frac{dp}{dt} + p\right). \tag{29}$$

Comparing this with equation (28) gives

$$\begin{aligned} L_1 &= (\lambda_q - \lambda_p)\frac{8\rho L}{\pi R^2} \\ R_1 &= \left(\frac{\lambda_q}{\lambda_p} - 1\right)\frac{8\mu L}{\pi R^4} \\ R_2 &= \frac{8\mu L}{\pi R^4}. \end{aligned} \tag{30}$$

Note that our derivations of the differential equations (25) and (28) were based on including only the first term from the sum on the right hand-side of equation (14).

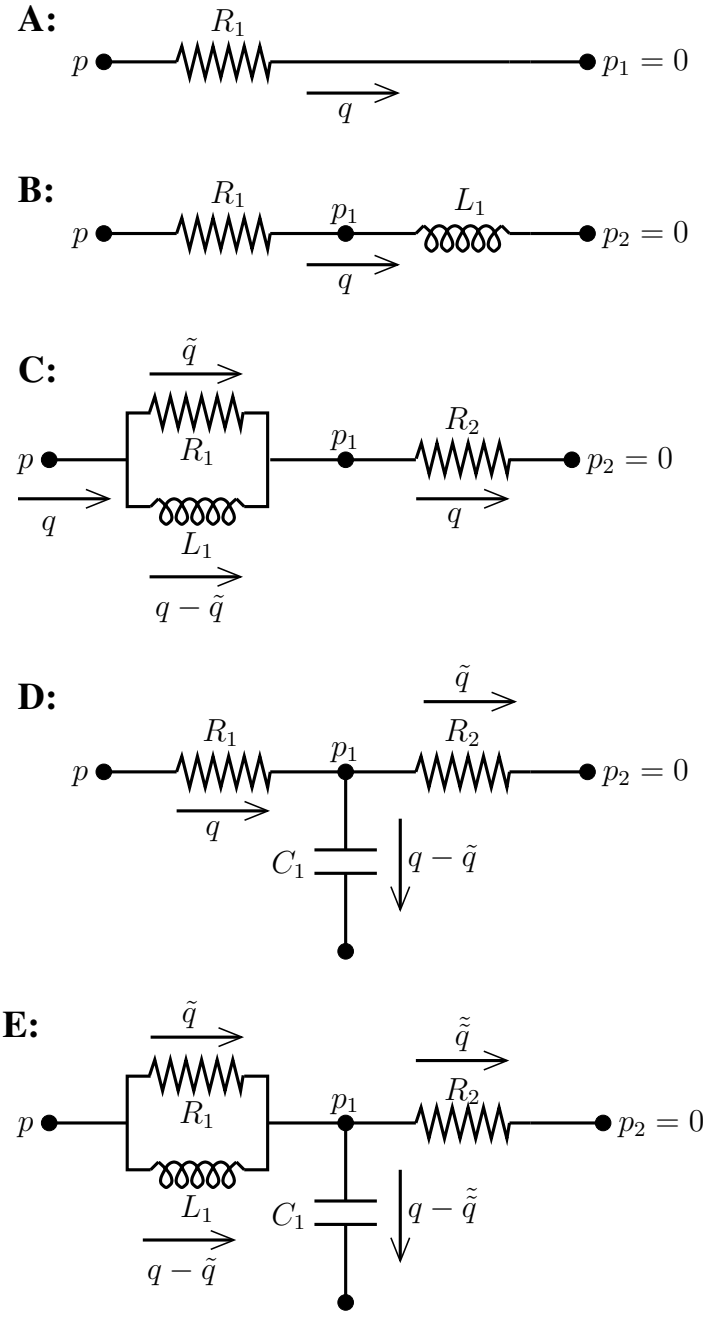

FIGURE 3. Lumped models: **A:** A resistor and an inductor. **B:** Two resistors and an inductor. **C:** Three-element windkessel model with two resistors and a capacitor. **D:** Four-element windkessel model with two resistors, an inductor, and a capacitor.

For vessels with a radius $R > 0.5$ cm, as discussed earlier, it is necessary to use the second-order model in equations (19) or (24). Upon examining this equation

it becomes clear that the coefficients in front of both second-order derivatives are small and can thus easily be neglected. In addition, the first-order derivative of p has a small coefficient. So, neglecting these terms yields a differential equation in the same form as equation (23). The difference between the equation obtained from the second-order model and equation (23) is that the time-scale for λ_q will be changed from $\lambda_q = 1/\beta_1^2$ to $\lambda_q = \lambda_{q_1} + \lambda_{q_2} = (1/\beta_1^2 + 1/\beta_2^2)$, increasing λ_q from 0.1729 to 0.2057. Consequently, the parameter for L_1 in equation (27) will be increased, whereas the resistance parameter R_1 will remain unchanged. Including the first-order derivative in p (the largest of the terms that were neglected) will yield an equation of the form of equation (18), where $\lambda_q = \lambda_{q_1} + \lambda_{q_2} = 0.2057$ and $\lambda_p = \lambda_{p_1} + \lambda_{p_2} = 0.0392$. The analogous circuit is the one shown in Fig. 3C with equation (29). The parameters in equations (30) would be modified such that the inductor L_1 would be slightly bigger, the resistance R_1 significantly smaller, but the resistance R_2 would remain unchanged. Including the second-order derivative in q would amount to inserting a second inductor in series with the second resistance R_2 in Fig. 3C. Reflecting on our analysis above of the second-order model, it is our belief that for vessels with a radius smaller than 1.5 cm it is not necessary to include terms of higher than second order even though the time-scale for p may increase, since the coefficients of high-order derivatives in the differential equation will be small. For vessels with a radius larger than 1.5 cm, we believe, as stated in the previous section, that a higher-order model becomes necessary. In fact we would recommend modeling such large vessels with a one-dimensional fluid dynamics model.

It should be noted that the two differential equations models discussed above are both based on flow in a rigid vessel. The arteries are compliant; so, as discussed in the introduction to this section, elasticity has to be included in our model. Including elasticity is not trivial if the goal is to derive lumped models directly from the fluid dynamic equations. In the work by Bergel in [5], a continuity equation is added, however as discussed in section II.C these considerations do not lead to ordinary differential equations that can be represented by circuits including capacitors. In other words, it is possible to derive equations with compliance, but not to obtain the very popular windkessel models. One way to account for the effect of elasticity effects is by superposition of the results for the rigid vessel with a compliant component represented by a capacitor in either of the models in Fig. 3B or C (or even A, if the small resistive vessels are also known to be compliant such as the rat aorta). In fact, the most promising lumped model for blood flow and pressure in the systemic arteries is the four-element windkessel model (see Fig. 3E) obtained by adding a capacitor to the circuit in Fig. 3C.

3.2. **Windkessel models.** In the following we relate the differential equations we have obtained to the popular windkessel model, and in the next section we provide a general review on how compliance has generally been included within lumped models.

One noteworthy feature is that the three-element windkessel model of Fig. 3D [10, 16, 21, 28, 30, 35] gives rise to a differential equation of the same form as equation (18), except the terms have a significantly different meaning. The equation for this circuit is:

$$\frac{R_1 R_2 C_1}{R_1 + R_2}\frac{dq}{dt} + q = \frac{1}{R_1 + R_2}\left(R_2 C_1 \frac{dp}{dt} + p\right),$$

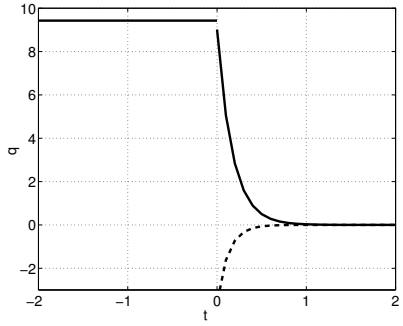

FIGURE 4. Flow as a function of time for a pressure drop p at time $t = 0$. The dotted curve is for the windkessel model and the solid curve is for the rigid vessel.

which also can be written in the form of equation (18):

$$\lambda_q \frac{dq}{dt} + q = \alpha \left(\lambda_p \frac{dp}{dt} + p \right).$$

Integrating this equation to solve for $q(t)$ gives:

$$q = \int_{-\infty}^{t} \frac{\alpha}{\lambda_q} \left(1 - \frac{\lambda_p}{\lambda_q} \right) e^{-(t-\tilde{t})/\lambda_q} p(\tilde{t}) \; d\tilde{t} + \alpha \frac{\lambda_p}{\lambda_q} p.$$

The above analysis is similar to the one carried out by Bird et al. [6] for viscoelastic flow.

Now, consider the response of the flow to a sudden pressure drop occurring at time $t = 0$:

$$p = \begin{cases} p_0 & \text{for} \quad t \leq 0 \\ 0 & \text{for} \quad t > 0. \end{cases}$$

The above equation for q for $t > 0$ reduces to

$$q = \alpha \left(1 - \frac{\lambda_p}{\lambda_q} \right) e^{-t/\lambda_q}. \tag{31}$$

The fundamental difference between the three-element windkessel model and the rigid vessel lumped model lies in the relation between the relaxation time λ_q and the retardation time λ_p. For the rigid vessel model, the retardation time is significantly smaller than the relaxation time ($\lambda_p \ll \lambda_q$), whereas for the three-element windkessel model the relaxation time is smaller than the retardation time ($\lambda_q < \lambda_p$). As a result the response q will have the form shown in Fig. 4. The important point to note is that for the rigid vessel the flow will always be positive (see solid line in Fig. 4). It will start at $\pi p_0/8$, and at $t = 0$ it will suddenly jump to $\pi p_0(1-\lambda_p/\lambda_q)/8$, from which it will decrease exponentially to zero. The reason for the initial jump is that when considering a step change in pressure that forces the flow, that step change will result in a delta-function forcing in the equation for q and hence an impulsive change in flow. For the three-element windkessel model, where $\lambda_p > \lambda_q$, the term in the parentheses in equation (31) becomes negative. Therefore, at $t = 0$ the flow will jump to a negative value and then increase exponentially to zero (dotted line in Fig. 4). The latter is a consequence of the capacitor: consider an elastic vessel at an initially high pressure p_0 where the pressure is suddenly turned off at

$t = t_0$. As a result the vessel will try to shrink and the flow could reverse. A similar phenomenon cannot take place in a rigid vessel.

Therefore, although the derivations of the rigid vessel lumped model and the three-element windkessel model lead to a differential equation of the same form, they cannot be interpreted the same way. In fact, if one tries to match the coefficients of the windkessel model to the ones from the rigid vessel model one will end up with a negative resistance and compliance. However, the NS-based derivation of the rigid vessel lumped model can provide information on the two resistances and the inductance, leaving just one parameter (the capacitance) that needs to be found from studying the properties of the arterial wall.

3.3. **Compliance Models.** None of the models discussed in the previous sections included elasticity, which in the circuit analogies amounts to adding capacitors. Several suggestions and derivations of lumped models are based on fluid flow in elastic vessels, two such models are [5, 15]. In this section we provide a summary of how compliance can be treated by reviewing the work discussed by Cheer and Keener. These are, to our knowledge, the only attempts to include compliance in these simplified models.

The model discussed by Keener and Sneyd departs from equation (1) by simply assuming that the pressure is a function of time only. That is, the inertial and viscous terms in the momentum equation are neglected altogether, yielding a uniform pressure within the vessel, which is assumed to be compliant. When combined with the equation for conservation of volume this yields

$$c\frac{dp}{dt} + A\frac{\partial u}{\partial x} = 0, \tag{32}$$

where it is assumed that $A(p) = A_0 + cp$, in which c is a local compliance. Solving for $u(x,t)$ by integrating from $x = 0$ to $x = L$ and multiplying by A_0, the cross-sectional area at zero transmural pressure, gives

$$q(t) = \theta(p)\frac{dp}{dt} + \frac{p}{R}. \tag{33}$$

Equation (33) corresponds to the two-element windkessel model, where the compliance of the vessel is given by

$$\theta(p) = \int_0^L \frac{A_0 c}{A_0 + cp} dx,$$

the inflow into the vessel is given by $q(t) = A_0 u(0,t)$, and the resistance R acting on the flow out of the vessel is given by $A_0 u(L,t) = p/R$. This model can also be obtained by adding a capacitor to equation (21) represented by the circuit shown in Fig. 3A.

To our knowledge, a similar derivation has not been made for either the three- or the four-element windkessel models. These models can be obtained by simply adding a capacitor to the circuit shown in Fig. 3C. The four-element windkessel model (Fig. 3E) can be obtained directly, while the three-element model (Fig. 3D) can be obtained by letting $L_1 \to \infty$, in which case all the flow will go through the resistance R_1 and none will go through the inductor. The equation for the four-element windkessel model (see Fig. 3E) is given by

$$C_1 L_1 R_1 R_2 \frac{d^2 q}{dt^2} + L_1(R_1 + R_2)\frac{dq}{dt} + R_1 R_2 q = C_1 L_1 R_2 \frac{d^2 p}{dt^2} + (L_1 + C_1 R_1 R_2)\frac{dp}{dt} + R_1 p. \tag{34}$$

Comparing this model with the one without the capacitance it is seen that the added capacitance gives rise to terms involving second-order derivatives in both p and q as well as an additional contribution to the coefficient of the first-order derivative of p.

Letting $L_1 \to \infty$ and integrating once with respect to t yield the differential equation for the three-element windkessel model:

$$C_1 R_1 R_2 \frac{dq}{dt} + (R_1 + R_2)q = C_1 R_2 \frac{dp}{dt} + p. \tag{35}$$

Alternatively, letting $R_1 \to \infty$ in equation (34) gives a model similar to the one shown in Fig. 3B with an added capacitor. This model can be written as

$$C_1 L_1 R_2 \frac{d^2q}{dt^2} + L_1 \frac{dq}{dt} + R_2 q = C_1 R_2 \frac{dp}{dt} + p. \tag{36}$$

Finally, a last approach to add compliance is the one suggested by Berger in [5]. In this paper, the point of departure is the axisymmetric flow in a vessel as described in equation (1) combined with equation (32) accounting for conservation of volume. In the derivation by Berger, viscosity and inertance are both included. In the equation for conservation of volume leakage through the vessel is also allowed, which is actually essential to the derivation. This leakage should be interpreted as the amount of blood lost due to vessels branching off from the vessel we study. Integrating the Womersley equation (1) over the cross-sectional area, assuming a Poiseuille velocity profile, and adding leakage to equation (32) for conservation of volume give:

$$\begin{aligned} -\frac{\partial p}{\partial x} &= \frac{\rho}{A}\frac{\partial q}{\partial t} + \frac{8\mu}{\pi R^4} q \\ -\frac{\partial q}{\partial x} &= \frac{\partial A}{\partial p}\frac{\partial p}{\partial t} + w' p \end{aligned}$$

where $\partial A/\partial p$ is the compliance and w' is the leakage per unit length which is equivalent to conductance. Instead of computing the lumped equation directly from the circuit, the analogy to signal transmission through a uniform cable is used. In this analogy pressure is equivalent to voltage, flow to current, ρ/A to inductance per unit length, $8\mu/\pi R^4$ to resistance. With the above interpretation the equations above can be represented by the circuit shown in Fig. 5. The equations for this circuit are given by:

$$\begin{aligned} p - p_1 &= R_1 q + L_1 \frac{dq}{dt} \\ C_1 \frac{dp_1}{dt} &= q - \tilde{q} \\ p_1 - 0 &= \frac{1}{G_1}\tilde{q}. \end{aligned}$$

Eliminating p_1 and $\tilde{q}$ gives

$$C_1 \frac{dp}{dt} + G_1 p = C_1 L_1 \frac{d^2q}{dt^2} + (C_1 R_1 + L_1 G_1)\frac{dq}{dt} + (1 + R_1 G_1)q.$$

Note that G_1 can be interpreted as a conductance for the leakage current. Its inverse plays the same role as the resistance R_2 would in Fig. 3D or 3E. If G_1 is set to zero (no leakage through the wall) or the corresponding resistance R_2 goes to infinity, the model fails because the flow path would end in the capacitor and as a result there will be no net flow through the system. In other words, it might be

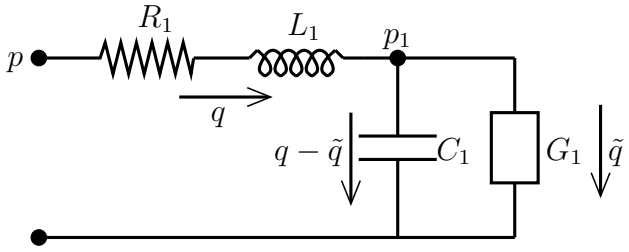

FIGURE 5. Circuit obtained from the model by Berger. The lumped model represented by this circuit is based on the fluid flow in an elastic vessel, with leakage through the wall.

better to interpret $1/G_1$ as the peripheral resistance and always keep it in Berger's model. If G_1 is replaced with $1/R_2$ in the last equation, we arrive at a circuit which is second order in flow q and first order in pressure p. This is similar to equation (36) although the latter only has one resistance rather than two.

In summary we conclude that if compliance is to be included in the fluid dynamic derivation, there is to our knowledge no simple way to obtain a lumped model without making a number of assumptions. One must assume that the fluid is inviscid and that the inertia is negligible, or simply add a capacitor to one of the models derived for flow in a rigid vessel, or allow for leakage through the vessel wall. In any case, based on our analysis of the time-scales lumped models are mainly useful for studying flow in the smaller vessels with a radius less than 0.5 cm.

4. **Discussion.** In this paper we have derived a number of lumped models based on the axisymmetric time-dependent fluid flow equation for a rigid vessel also known as Womersley's equation. Assuming that the vessel is rigid and the flow is laminar, we were able to make a series expansion of the solution of Womersley's equation to obtain a number of lumped models. Based on studying the characteristic time-scales for this problem we can conclude that for arteries with a radius smaller than 0.2 cm it is possible to assume that pressure is proportional to flow. The circuit representing such a vessel would simply contain a resistance and no other elements. In other words, effects due to inertia can completely be ignored. Since such small arteries are typically rigid (although there are exceptions) but do provide resistance, it will be unnecessary to add a capacitor to the model to account for elasticity. However, as shown by Keener and Sneyd [15] it is possible to incorporate elasticity using the two-element windkessel model; that is, by adding a capacitor to the circuit shown in Fig. 3A. It should be noted that the derivation by Keener and Sneyd is somewhat artificial, it includes neither viscosity nor inertia.

For vessels with a radius between 0.2 and 0.5 cm, it is necessary to add additional elements to the model. The minimum model that would take some of the effect of inertance into account is the first-order model (23) that includes a resistor and inductor in series (see Fig. 3B). As for the very small vessels, this model can be obtained either from including an additional term in the residue method for the inversion integral, but neglecting the small retardation time.

For vessels with a radius larger than 0.5 cm, we conclude that a higher-order model should be used. By higher-order, we mean a model that includes contributions from more of the residues. If two terms are included, one can still ignore

the second-order derivative in pressure, yielding a model with two derivatives (i.e. second-order) in flow and one derivative (i.e. first order) in pressure. A circuit that can represent this model would be equivalent to the fourth-order windkessel model, but without the capacitor.

Finally, for vessels with a radius larger than 1.5 cm, more terms in the expansion are needed to get an accurate lumped model of the flow. Therefore, we conclude that for large vessels (e.g., the aorta) it would be more appropriate to use distributed models (one-, two-, or three-dimensional models) for simulating blood flow and pressure. This fits well with our intuitive understanding that in such vessels the fluid dynamics is more complex and spatially varying. In that case, one option is to use the windkessel model as a boundary condition at the outflow for the large vessels, as discussed for instance in the papers [19, 27].

Our derivation provides some justification for the recent observation that the four-element windkessel model (including inductance) suggested by [29] fits the data better than the three-element windkessel model. It should be noted that lumped models are frequently used to describe the cardiovascular system as a whole, including all vessels from the aorta to the arterioles. In our derivations, however, we considered flow in a single vessel and its corresponding lumped description. In our view, a more accurate but obviously more complex model of the systemic arteries can be constructed by considering the bifurcating network of branched arteries and describing each element in that network by its appropriate lumped model. Since coupling such low-order models will quickly result in a high-order model, it may be justified to simplify the description and use a low-order model for the network as a whole. It is evident though that by coupling individual elements that possess resistance, compliance and inductance, the whole network should also possess such elements in its overall lumped description.

Acknowledgements. Mette Olufsen was supported by a modular grant from the National Institute of Health #R03-AG20833-01 and by a Faculty Research and Development Fund Grant from North Carolina State University SPS #0064-8604.

Appendix A. **Residues for** $M(t)$**.** The residues of $(K(s)/s)e^{st}$ are computed herein. To do so it is advantageous to write

$$\frac{K(s)}{s}\,e^{st} = \frac{\pi}{s^2}\left(\frac{i\sqrt{s}J_0(i\sqrt{s}) - 2J_1(i\sqrt{s})}{i\sqrt{s}J_0(i\sqrt{s})}\right)e^{st}. \tag{37}$$

From the above expression, it can be seen that $(K(s)/s)\,e^{st}$ has a simple pole at $s = 0$ and an infinite number of poles where $J_0(i\sqrt{s}) = 0$. The residue at the simple pole at $s = 0$ can be found to be $\pi/8$ by series expansion for small values of s:

$$\begin{aligned}
K(s) &= \frac{\pi}{s}\left(1 - \frac{2J_1(i\sqrt{s})}{i\sqrt{s}J_0(i\sqrt{s})}\right) \\
&= \frac{\pi}{s}\left(1 - \left[1 + \frac{(i\sqrt{s})^2}{8} + \frac{(i\sqrt{s})^4}{48} + \frac{11(i\sqrt{s})^6}{3072} + \ldots\right]\right) \\
&= \frac{\pi}{s}\left(\frac{s}{8} + \frac{s^2}{48} - \frac{11\,s^3}{3072} + \mathcal{O}(s^4)\right) \\
&= \frac{\pi}{8} - \frac{\pi s}{48} + \frac{11\pi s^2}{3072} + \mathcal{O}(s^3).
\end{aligned}$$

The remaining residues (where $J_0(i\sqrt{s}) = 0$) can be found as follows: denote the zeros of $J_0(\beta)$ by $\beta_n, n = 1, 2, 3, \ldots$, then the poles for $(K(s)/s)\, e^{st}$ are at 0 and at points where

$$\beta_n = i\sqrt{s_n} \qquad \Leftrightarrow \qquad s_n = -\beta_n^2.$$

Starting with equation (37) and evaluating the residue at $s_n = -\beta_n^2$ yields:

$$\begin{aligned} \mathrm{Res}(s_n) &= \frac{\pi}{\beta_n^5}\left[\frac{-2J_1(\beta_n)}{\frac{d}{ds}J_0(i\sqrt{s})\big|_{s=-\beta_n^2}}\right] e^{-\beta_n^2 t} \\ &= \frac{\pi}{\beta_n^5}\left[\frac{-2J_1(\beta_n)}{J_1(\beta_n)/(2\beta_n)}\right] e^{-\beta_n^2 t} \\ &= \frac{-4\pi e^{-\beta_n^2 t}}{\beta_n^4}. \end{aligned}$$

REFERENCES

[1] M. Abramowitz and I. A. Stegun, *Handbook of Mathematical Functions*. New York, NY: Dover Publications, 1970, pp. 409.

[2] H. B. Atabek and H. S. Lew, "Wave propagation through a viscous incompressible fluid contained in an initially stressed elastic tube," *Biophys. J.*, vol. 6, pp. 481-503, 1966.

[3] H. B. Atabek, "Wave propagation through a viscous fluid contained in a tethered, initially stressed, orthotropic elastic tube," *Biophys. J.*, vol. 8, pp. 626-649, 1968.

[4] A. P. Avolio, "Multi-branched model of the human arterial system," *Med Biol. Eng. Comput.*, vol. 18, pp. 709-718, 1980.

[5] S. A. Berger, 'Flow in large blood vessels," in *Fluid Dynamics in Biology, Contemporary Mathematics*, vol 141, A. Y. Cheer and C. P. van Dam, Ed., Providence, RI: Am. Math. Soc., 1993, pp. 479-518.

[6] R. B. Bird, R. C. Armstrong, and O. Hassager, *Dynamics of Polymeric Liquids, Volume 1: Fluid mechanics*, 2nd ed, New York, NY: John Wiley & Sons, 1987, pp. 261-262.

[7] P. Broemser and O. R. Ranke, "Über die messung des schlagvolumens des herzens auf umblutigem weg," *Z. Biol.*, vol. 90, pp. 467-507, 1930.

[8] C. G. Caro, T. J. Pedley, R. C. Schroter, and W. A. Seed, *The Mechanics of the Circulation*. Oxford, U. K.: Oxford University Press, 1978.

[9] M. Danielsen and J. T. Ottesen, "A dynamical approach to the baroreceptor regulation of the cardiovascular system," in *Proc. 5th Int. Symp., Symbiosis '97*, 1997, pp. 25-29,

[10] R. Fogliardi, "Comparison of linear and nonlinar formulations of the three element windkessel model," *Am. J. Physiol.*, vol. 271, pp. H2661-H2668, 1996.

[11] O. Frank, "Die grundform des arteriellen pulses. Erste Abhandlung, Mathematische analyse," *Z. Biol.*, vol. 37, pp. 483-526, 1899.

[12] U. Gessner, "Vascular input impedance," In *Cardiovascular Fluid Dynamics*, vol. 1 ch 10, D. H. Bergel, Ed, London, U. K.: Academic Press, London, 1972.

[13] S. Hales, *Statical Essays: II Haemostaticks*. London, U. K.: Innays and Manby, Reprinted by New Yourk, NY: Hafner, 1733.

[14] T. J. R. Hughes and J. Lubliner, "On the one-dimentional theory of blood flow in the larger vessels," *Math. Biosciences*, vol. 18, pp. 161-170, 1973.

[15] J. Keener and J. Sneyd, *Mathematical Physiology, vol. 8th of Interdisciplinary Applied Mathematics*. New York, NY: Springer Verlag, 1998.

[16] B. Lambermont, P. Gerard, O. Detry, P. Kohl, P. Potty, J. O. Defraigne, V. D'Orio, and R. Marcelle, "Comparison between three- and four element windkessel models to characterize vascular properties of pulmonary circulation," *Arch. Physol. Biochem.*, vol. 105, pp. 625-632, 1997.

[17] J. Larsen and S. A. Pedersen, "Mathematical Models Behind Advanced Simulators in Medicine," in *Mathematical Modelling in Medicine, vol. 71 of stud. health tech. inf.*, J. T. Ottesen and M. Danielsen, Ed., pp. 203–217. Roskilde, Denmark: IOS Press, 2001.

[18] J. Lighthill, "Physiological fluid dynamics: A Survey," *J. Fluid. Mech.*, vol. 52(part 3), pp. 475-497, 1972.

[19] M. S. Olufsen, "Structured tree outflow condition for blood flow in larger systemic arteries," *Am. J. Physiol.*, vol. 276, pp. H257-H268, 1999.
[20] M. S. Olufsen, C. S. Peskin, J. Larsen, and A. Nadim, "Derivation and validation of physiologic outflow condition for blood flow in the systemic arteries," *Ann. Biomed. Eng.*, vol. 28, pp. 1281-1299, 2000.
[21] M. S. Olufsen, A. Nadim, and L. A. Lipsitz, "Dynamics of cerebral blood flow regulation explained using a lumped parameter model," *Am. J. Physiol.*, vol. 282, pp. R611-R622, 2002.
[22] J. T. Ottesen, "Modelling the baroreflex-feedback mechanism with time-delay," *J. Math. Biol.*, vol. 36, pp. 41-63, 1997.
[23] J. T. Ottesen, "Nonlinearity of baroreceptor nerves," *Surv. Math. Ind.*, vol. 7, pp. 187-201, 1997.
[24] T. J. Pedley, *The Fluid Mechanics of Large Blood Vessels* Cambridge, U. K.: Cambridge University Press, 1980.
[25] C. M. Quick, D. L. Young, and A. Noordergraaf, "Infinite number of solutions to the hemodynamic inverse problem," *Am. J. Physiol.*, vol. 280, pp. H1472-H1479, 2001.
[26] P. Segers, F. Dubois, D. DeWachter, and P. Verdonck, "Role and relevancy of a cardiovascular simulator," *J. Cardiovasc. Eng.*, vol. 3, pp. 48-56, 1998.
[27] N. Stergiopulos, D. F. Young, and T. R. Rogge, "Computer simulation of arterial flow with applications to arterial and aortic stenosis," *J. Biomech.*, vol. 25, pp. 1477-1488, 1992.
[28] N. Stergiopulos, J. J. Meister, and N. Westerhof, "Evaluation of methods for estimation of total arterial compliance," *Am. J. Physiol.*, vol. 268, pp. H1549-H1554, 1995.
[29] N. Stergiopulos, B. E. Westerhof, and N. Westernof, "Total arterial inertance as the fourth element of the windkessel model," *Am. J. Physiol.*, vol. 276, pp. H81-H88, 1999.
[30] G. P. Toorop, N. Westerhof, and G. Elzinga, "Beat-to-beat estimation of peripheral resistance and arterial compliance during pressure transients," *Am. J. Physiol.*, vol. 21, pp. H1275-H1283, 1987.
[31] S. M. Toy, J. Melbin, and A. Noordergraaf, "Reduced models of arterial systems," *IEEE Trans. Biomed. Eng.*, vol. 32(2), pp. 174-176, 1985.
[32] M. Ursino, "A mathematical model of the carotid-baroreflex control in pulsatile conditions," *Surv. Math. Ind.*, vol. 7, pp. 203-220, 1997.
[33] M. Ursino, "A mathematical model of the carotid baroregulation in pulsating conditions," *IEEE Trans. Biomed. Eng.*, vol. 46, pp. 382-392, 1999.
[34] N. Westerhof, F. Bosman, C. J. DeVries, and A. Noordergraaf, "Analog studies of the human systemic arterial tree," *J. Biomech.*, vol. 2, pp. 121-143, 1969.
[35] N. Westerhof, G. Elzinga, and P. Sipkema, "An artificial system for pumping hearts," *J. Appl. Physiol.*, vol. 31, pp. 776-781, 1971.
[36] J. R. Womersley, "Oscillatory flow in arteries: The constrained elastic tube as a model of arterial flow and pulse transmission," *Phys. Med. Biol.*, vol. 2, pp. 178-187, 1957.
[37] J. R. Womersley, "An elastic tube theory of pulse transmission and oscillatory flow in mammalian arteries," Wright Air Development Center (WADC), Air Research and Development Command, United States Air Force, Wright-Patterson Air Force Base, Ohio, *WADC TR* 56-614, 1957.

Received on Jan. 9, 2004. Revised on Feb. 18, 2004.

E-mail address: msolufse@math.ncsu.edu
E-mail address: nadim@kgi.edu